ORIGINAL INVESTIGATION

Subchronic memantine induced concurrent functional disconnectivity and altered ultra-structural tissue integrity in the rodent brain: revealed by multimodal MRI

S. Sekar · E. Jonckers · M. Verhoye · R. Willems · J. Veraart ·
J. Van Audekerke · J. Couto · M. Giugliano · K. Wuyts · S. Dedeurwaerdere ·
J. Sijbers · C. Mackie · L. Ver Donck · T. Steckler · A. Van der Linden

Abstract

Background An effective NMDA antagonist imaging model may find key utility in advancing schizophrenia drug discovery research. We investigated effects of subchronic treatment with the NMDA antagonist memantine by using behavioural observation and multimodal MRI.

Methods Pharmacological MRI (phMRI) was used to map the neuroanatomical binding sites of memantine after acute and subchronic treatment. Resting state fMRI (rs-fMRI) and diffusion MRI were used to study the changes in functional connectivity (FC) and ultra-structural tissue integrity before and after subchronic memantine treatment. Further corroborating behavioural evidences were documented.

Results Dose-dependent phMRI activation was observed in the prelimbic cortex following acute doses of memantine. Subchronic treatment revealed significant effects in the hippocampus, cingulate, prelimbic and retrosplenial cortices. Decreases in FC amongst the hippocampal and frontal cortical structures (prelimbic, cingulate) were apparent through rs-fMRI investigation, indicating a loss of connectivity. Diffusion kurtosis MRI showed decreases in fractional anisotropy and mean diffusivity changes, suggesting ultra-structural changes in the hippocampus and cingulate cortex. Limited behavioural assessment suggested that memantine induced behavioural effects comparable to other NMDA antagonists as measured by locomotor hyperactivity and that the effects could be reversed by antipsychotic drugs.

Conclusion Our findings substantiate the hypothesis that repeated NMDA receptor blockade with nonspecific, noncompetitive NMDA antagonists may lead to functional and ultra-structural alterations, particularly in the hippocampus and cingulate cortex. These changes may underlie the behavioural effects. Furthermore, the present findings underscore the utility and the translational potential of multimodal MR imaging and acute/subchronic memantine model in the search for novel disease-modifying treatments for schizophrenia.

S. Sekar · E. Jonckers · M. Verhoye · J. Van Audekerke ·
A. Van der Linden
Bio-Imaging Lab, Department of Biomedical Sciences,
University of Antwerp, Campus Drie Eiken, D.UC.109,
Universiteitsplein 1, 2610, Wilrijk, Belgium

S. Sekar (✉) · R. Willems · L. Ver Donck · T. Steckler
Neuroscience Discovery, Janssen Research and Development,
Beerse, Belgium
e-mail: sekar.sakthivel@ua.ac.be

J. Veraart · J. Sijbers
Vision Lab, University of Antwerp, Antwerp, Belgium

J. Couto · M. Giugliano
Theoretical Neurobiology, University of Antwerp,
Antwerp, Belgium

K. Wuyts · C. Mackie
ADME/Tox, Janssen Research and Development, Beerse, Belgium

S. Dedeurwaerdere
Translational Neuroscience, University of Antwerp,
Antwerp, Belgium

Present Address:
S. Sekar
SBIC, A*Star, Biopolis, Singapore

Keywords NMDA antagonists · Memantine · Locomotor activity · Pharmacological MRI · Resting state fMRI · DTI/DKI · Cingulate cortex · Hippocampus · Schizophrenia · Antipsychotic drugs

Introduction

In vivo translational imaging, such as magnetic resonance imaging (MRI) and positron emission tomography (PET), has gained substantial interest in advancing drug discovery research (Fox et al. 2009; Wong et al. 2009). Functional, resting state and diffusion imaging are specialised MRI protocols particularly useful in CNS drug discovery research. While functional magnetic resonance imaging (fMRI) is extensively used to investigate central activity related to sensory or cognitive stimuli, a blood oxygenation level-dependent (BOLD) fMRI response can also be evoked when the brain is challenged by psychoactive compounds (Borsook et al. 2006). This technique is commonly referred to as pharmacological MRI (phMRI) (Borsook and Becerra 2010). Resting state fMRI (rs-fMRI), on the other hand, has the potential to investigate functional connectivity (FC) in the pharmacologically modulated brain in rodents (Bifone et al. 2010; Schwarz et al. 2007). Similarly, diffusion kurtosis imaging is particularly useful in characterising the ultrastructural tissue changes in disease models (Delgado y Palacios et al. 2011).

These neuroimaging methods therefore allow a better understanding on the neurobiological mechanisms underlying psychoactive drug effects. Briefly, mapping the neuroanatomical target sites and studying the subsequent adaptations across doses, treatment regimes and/or with a co-administration of a suitable agonist or antagonist allow for a better understanding on the mechanism of action of compounds in vivo (Sekar et al. 2010, 2011a, b).

The glutamatergic hypothesis of schizophrenia is supported by several lines of clinical evidence; this includes postmortem, genetic and human psychosis modelling (Krystal et al. 1994; Malhotra et al. 1997). In this context, NMDA antagonists, such as ketamine or phencyclidine (PCP), can induce a wide range of positive, negative and cognitive symptoms in healthy volunteers that resemble those in patients with schizophrenia (Coyle and Tsai 2004; Mechri et al. 2001a). When administered to patients, the exacerbated psychotic symptoms have a striking similarity to the symptoms during their usual schizophrenic episodes (Bubeníková-Valesová et al. 2008; Mechri et al. 2001a, b).

Using in vivo phMRI, Gozzi et al. (2008a) investigated the modulatory effects of PCP along with co-treatment by endogenous and exogenous agonists on the BOLD signal in rats. Ketamine was reported to produce a dose-dependent increase in the BOLD-MR signal localised in the frontal, hippocampal, cortical and limbic areas, which correlated with the pharmacodynamic profile of the drug (Littlewood et al. 2006a). In a parallel study involving stereoisomers of ketamine [(R−), (S+)], comparable activation was observed

in cortical and hippocampal regions (Littlewood et al. 2006b). Further studies in humans using [18F]-fluorodeoxyglucose and PET imaging showed that a subanaesthetic dose of ketamine induced a bilateral increased metabolic activity in regions of the prefrontal cortex (Langsjo et al. 2004) and a reduced cerebral blood flow in the hippocampus (Mechri et al. 2001a; Langsjo et al. 2003, 2004). Similar responses have been reported using the NMDA antagonist MK-801 in the limbic and frontal cortex in a phMRI study; this correlated with changes in 2-deoxyglucose (2-DG) autoradiography of regional brain glucose metabolism in rats (Houston et al. 2001).

Memantine is a low affinity, high-voltage-dependent noncompetitive antagonist of the NMDA receptor; it has fast blocking–unblocking kinetics, which facilitates a rapid clearance from the NMDA channel during physiological activation, yet blocking the receptors during peak activity (Danysz et al. 2000). Our earlier work demonstrated robust and reproducible increases in brain glucose metabolism after acute memantine treatment in mice, and this effect was reversible with antipsychotic drugs (Dedeurwaerdere et al. 2011).

Despite profound differences in pharmacokinetics, behavioural profiling of memantine in rats has demonstrated similar disruptions in spontaneous and reward-motivated psychomotor behaviours between ketamine and memantine (Gilmour et al. 2009). However, ketamine has been classified as a controlled drug, and PCP was withdrawn from the clinical formulary because of abuse liability and neurotoxicity concerns (Olney et al. 1991, 1995), whereas memantine is safely used in the clinic, to improve cognitive function in patients with Alzheimer's disease (Peskind et al. 2006; Winblad et al. 2007). Memantine is well tolerated, has linear kinetics and 100 % bioavailability (following oral dosing) (Aerosa et al. 2005; Wilcock et al. 2002). Moreover, an advantage of memantine compared to ketamine is its long biological half-life known to be around 2–4 h (Alley et al. 2010). Hence, an MRI imaging model using memantine would be useful to explore novel disease-modifying treatments across preclinical and clinical settings in vivo. To our knowledge, this is the first multimodal imaging study investigating memantine in rats.

The aim of this study was (a) to evaluate the effects of acute and subchronic administration of memantine on brain activation as well as functional and anatomical connectivity using multimodal imaging techniques in rats and (b) to correlate these with behavioural responses. We have used phMRI to map the neuroanatomical target sites of memantine and to study the subsequent adaptation in the BOLD response from acute to subchronic treatment. rs-fMRI was used to study FC among discrete brain structures apparent from the phMRI results. Finally, diffusion MRI was used to study the ultra-structural changes in the regions of interest.

Methods and materials

Animals

All procedures were conducted in compliance with the Belgian law (Royal Decree on the protection of laboratory animals, dd. April 6, 2010). The study protocols were approved by the institutional animal experimental ethical committees of Janssen Research & Development (Beerse, Belgium) and University of Antwerp (Antwerp, Belgium).

Male Lister Hooded rats were obtained from Charles River (Germany). Animals were housed in enriched individual ventilated cages in groups of four and habituated to environmental conditions for at least 5 days with food and water ad libitum (conditions: 12:12-h light/dark cycle, temperature, 20–24 °C and humidity 45–65 %). Mean body weight range at experimental day was 240–300 g. Rats were used only once in an experiment and euthanized afterwards.

Drugs and treatment groups

Behavioural experiments

Memantine was obtained from Manus Aktteva Biopharma (Ahmedabad, India); PCP, risperidone, haloperidol and olanzapine were synthesised at Janssen Research & Development (Beerse, Belgium). In the acute dose–response experiments, memantine or PCP was administered at doses of 10, 20 or 40 mg/kg intraperitoneally (IP) or 0.63, 1.25 or 2.5 mg/kg subcutaneously (SC), respectively. Based on the inference from these acute dose–response experiments and from the historical data from studies in Janssen Research & Development, subjects received memantine (20 mg/kg/day, IP) or PCP (1.25 mg/kg/day, SC) once daily for five consecutive days. Two to three days after the last subchronic administration, rats were challenged acutely with memantine (20 mg/kg, IP) or PCP (2.5 mg/kg, SC), respectively. Saline was used as the vehicle to dissolve memantine or PCP.

Haloperidol was dissolved in saline + 1 equivalent tartaric acid (=0.5 ml of 1 N tartaric acid per 10-mg compound); olanzapine and risperidone were dissolved in saline + 2 equivalents tartaric acid. The vehicle was administrated in the control group. Drugs were administered 30 min prior to acute challenge with memantine or PCP. All compound solutions were stored at room temperature in a closed container protected from light, and the injection volume was 10 ml/kg. The study involved 49 experimental groups: ten rats/group in acute and in subchronic memantine or PCP experiments and 12 rats/group in antipsychotic drug testing experiments. The experimental design of the behavioural experiments is provided in Table 1 (see Suppl. Material).

Imaging experiments

Acute phMRI experiments involved memantine administered in two doses (20 and 40 mg/kg IP). For subchronic testing, single daily injections of 20 mg/kg/day (IP) were used for five consecutive days. Saline was used as the vehicle for all preparations. Dose selection was based on our behavioural data and a previously published dose–response study to evaluate NMDA antagonist-induced 2-DG functional brain activations (Dedeurwaerdere et al. 2011).

It is worth mentioning that memantine has been safely used in the clinic; however, the therapeutic doses are in the order of at least five times lower than the 20-mg/kg dose utilised in this study (Parsons et al. 2007).
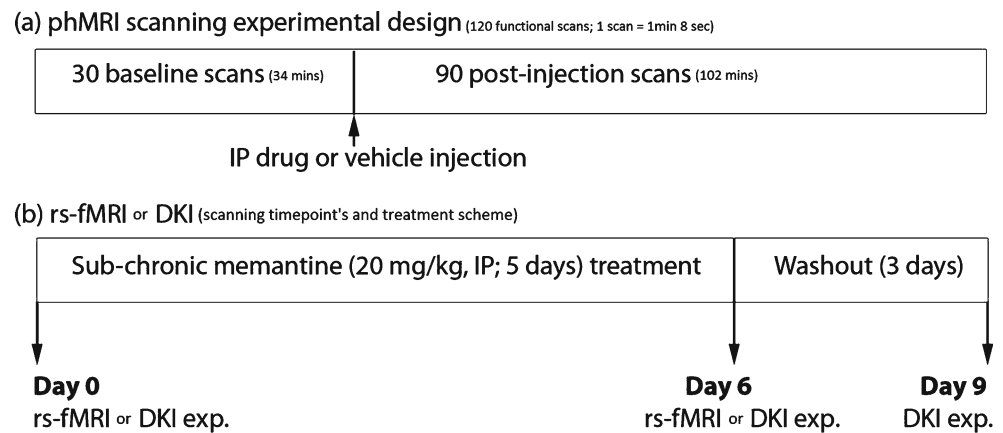
The study design and overview of the imaging experiments are provided in Table 1. Overview of the scanning experimental design and time points are provided in Fig. 1a, b. For phMRI measurements, the study involved five experimental groups (six rats in each group): acute memantine treatment dose 1, dose 2, controls (vehicle treated), subchronic memantine treatment (20 mg/kg, IP) and chronic control (vehicle treated).

For all phMRI experiments, a single IP administration of memantine or saline was used as the stimulus to generate a phMRI-BOLD response. Longitudinal resting state

Table 1 Study design and overview of the MRI experiments

Type of MRI modality	Treatment and dose	Number of subjects	Experimental design (longitudinal scanning)
phMRI	Acute memantine or vehicle (20 or 40 mg/kg, IP) treatment	6 per group	Individual groups ($n=3$)
phMRI	Subchronic memantine or vehicle (20 mg/kg, IP/ day–5 days) treatment	6 per group	Individual groups ($n=2$)
rs-fMRI	Subchronic memantine (20 mg/kg, IP/day–5 days) treatment	8 subjects	Same subject group scanned at 2 time points (pretreatment and posttreatment)
DKI	Subchronic memantine (20 mg/kg, IP/day–5 days) treatment	10 subjects	Same subject group scanned at 3 time points (pretreatment and posttreatment and post 3-day wash-out)

phMRI pharmacological MRI, *rs-fMRI* resting state functional MRI, *DKI* diffusion kurtosis imaging

Fig. 1 Experimental protocol of phMRI study (**a**) and rs-fMRI and DKI study (**b**)

(a) phMRI scanning experimental design (120 functional scans; 1 scan = 1min 8 sec)

| 30 baseline scans (34 mins) | 90 post-injection scans (102 mins) |

IP drug or vehicle injection

(b) rs-fMRI or DKI (scanning timepoint's and treatment scheme)

| Sub-chronic memantine (20 mg/kg, IP; 5 days) treatment | Washout (3 days) |

Day 0
rs-fMRI or DKI exp.

Day 6
rs-fMRI or DKI exp.

Day 9
DKI exp.

or diffusion MRI measurements were conducted before and after subchronic treatment in separate groups of eight or ten rats, respectively. In addition, diffusion measures were acquired after 3 days of wash-out. No drug/vehicle challenge was involved in the resting state and diffusion MRI measurements, as compared to phMRI measurements.

Pharmacokinetics experiments

Pharmacokinetics of memantine was determined in the plasma and brain after acute and subchronic treatment to correlate with responses in the MRI and behavioural studies. A single or 5-day repeated injection of memantine (20 mg/kg, IP) was given to treatment naïve animals ($n=3$/group), and subjects were sacrificed at 0.5, 1, 2, 4, 7 and 24 h postdose to collect blood and brain samples.

Locomotor activity (methods)

Apparatus

Locomotor activity (LMA) was measured by placing rats in black Perspex cylinders of ∅30 cm and 35-cm height with infrared light provided via the open circular area at the bottom. Live images captured by a CCD video camera (five frames/second) mounted 50 cm above each cylinder (12 in total) enabled image analysis software (Ethovision XT, Noldus, The Netherlands) to quantify total distance travelled, tracking areas for each cylinder were individually calibrated, and the X–Y coordinates of the centre of gravity of each subject as determined by the software per video frame were used to calculate the total distance travelled. All experiments were performed during the light cycle, between 0800 and 1700 hours.

Experimental procedure and data analysis

Animals were placed in the arenas for a 30-min habituation phase followed by 60 min after administration of an acute challenge with memantine, PCP or their vehicle. Total

distance travelled was cumulated over the habituation and challenge periods, respectively. Ethovision data were exported to MS Excel for graphing and imported in SPSS (IBM, US) for statistical analysis by unpaired t test or ANOVA with Dunnett's post hoc test as appropriate.

Multimodal MRI imaging (methods)

Subject preparation

Initially, rats were anesthetised with 3.5 % isoflurane (Isoflo®, Abbott Laboratories Ltd., USA) in a gas mixture of 30 % oxygen and 70 % nitrogen in an induction box, an IP catheter was placed for the drug challenge and positioned in a stereotaxic head-holding device as described previously (Sekar et al. 2011a, b). During phMRI or diffusion MRI data acquisition, maintenance of the anaesthesia was achieved using 0.9 to 2 % isoflurane. For the rs-fMRI experiment, the use of isoflurane is argued to be suboptimal (Williams et al. 2010); hence, the animals were sedated using medetomidine (Domitor, Pfizer, Germany), which has been reported to preserve functional connectivity (Pawela et al. 2009). Initially, a bolus of 0.05 mg/kg was injected SC, and isoflurane was discontinued after 5 min and then followed by a continuous infusion of medetomidine (0.1 mg/kg/h, SC). After the scanning procedure, medetomidine was antagonised by an injection of atipamezole (0.1 mg/kg, SC) (Antisedan, Pfizer, Germany) (Weber et al. 2006).

Uninterrupted physiological monitoring and maintenance was observed throughout the experiments, as described in Sekar et al. (2011a, b). Subject selection for scanning was counterbalanced across treatment/dosing groups, to have an even distribution across daylight time. Repeated scanning sessions in the same animal were planned, taking into account the diurnal rhythm.

Experimental protocol

All imaging experiments were performed on a 9.4T Biospec scanner (Bruker, Ettlingen, Germany) using a Bruker linear

transmit volume coil. An actively decoupled circular surface receiver coil was placed on top of the stereotaxically positioned flat skull of the rat. For rs-fMRI, a parallel receive surface array was used.

phMRI images were acquired using a gradient echo (GE) sequence (repetition time (TR), 1,048 ms; echo time (TE), 17 ms; field of view (FOV), 25×25 mm^2; matrix size, 64×64; slice thickness, 0.5 mm, 32 axial slices; and resolution, $0.39 \times 0.39 \times 0.5$ mm^3). One hundred twenty functional scans were acquired for each subject: 30 baseline (33 min) and 90 postinjection (100 min) scans (Fig. 1).

For rs-fMRI, a single shot gradient echo-planar imaging (EPI) sequence was used to obtain the images (TR, 2,000 ms; TE, 16 ms; FOV, 30×30 mm^2; matrix size, 128×128; slice thickness, 1 mm, 12 axial slices; resolution, $0.23 \times 0.23 \times 1$ mm^3; and bandwidth 400 kHz, 150 repetitions).

Diffusion MRI images were acquired using a spin echo (SE)-EPI sequence (TR, 10 s; TE, 24 ms; FOV, 35×23 mm^2; acquisition matrix, 96×64; zero filled to 128×64, 50 axial slices; and resolution, $0.28 \times 0.37 \times 0.5$ mm^3). Diffusion-weighted images were acquired with diffusion gradient pulse duration $\delta = 5$ ms; diffusion gradient separation $\Delta = 12$ ms; and b values 500, 1,000 and 2,800 s/mm^2 applied in 33, 88 and 178 noncollinear optimised directions, respectively.

Data analysis

Pharmacological MRI

Prior to statistical analysis, images were extensively preprocessed. The image time series from each subject was realigned using a least-square approach and rigid body spatial transformation to eliminate any potential motion related artefacts using SPM99. A single subject (from the experimental group) was randomly chosen as the template, and all subjects were spatially normalised to the template using a 12-parameter affine transformation based on the maximalization of the product of the likelihood function (derived from the residual squared difference) and the prior function (which is based on the probability of obtaining a particular set of zooms and shears) (Ashburner et al. 1997). Vascular masks, derived by applying a coefficient of variance threshold of 15 %, were used to suppress signal changes associated with macroscopic vessels, minimising the contamination of surrounding parenchyma associated with spatial smoothing as proposed and described by Hlustik et al. (1998); these masks were applied to all realigned volumes within the respective time series of each subject. Individual brain masks, generated using AMIRA software (Visage Imaging), were subsequently applied to each subjects' time series, which were Gaussian smoothed to impose a normal distribution, using a full width half maximum

(FWHM) kernel of $0.78 \times 0.78 \times 1$ mm^3 (twice the size of image resolution). A comparison between preinjection and postinjection scans ("off/on" model) was used to assess the main effect of the treatment, and parametric maps of statistical significance were obtained using a fixed effects general linear model, using SPM99, as previously described (Sekar et al. 2011a, b). Relative longer half-life of memantine compared to other NMDA antagonists (Alley et al. 2010) ensures elevated memantine concentrations for the duration of the imaging experiment. A comparison of preinjection and postinjection scans serves to be a suitable method of assessing the phMRI-BOLD responses. Global muscle signal intensities were determined for each subject and used as covariates, controlling for global drift effects (Lowe et al. 2008). Subject movement was considered by including the realignment parameters as a nuisance variable (covariates of no interest). Statistical significance for the statistical parametric maps (SPMs) was set at $p < 0.05$, corrected for multiple comparisons (using a random Gaussian field method, a statistically valid approach that would not be hobbled by the overly conservative assumptions of a standard Bonferroni correction). Group statistical parametric map for each treatment (overlaid onto anatomical structural images) displaying T-distribution of BOLD contrast changes after drug administration, with coloured pixels representing T-scores of significant increases and decreases between "pre" and "post" scans were determined. In order to investigate any systemic effect components in the data: general linear model univariate analysis of variance was conducted between subjects mean muscle signal intensities and the injection protocol (Lowe et al. 2008).

Resting state fMRI

Prior to FC assessment, an equally comparable/extensive preprocessing (as with the phMRI analysis) was conducted on the rs-fMRI data, using SPM8, that includes the following: realignment, normalisation, estimation of nonlinear deformations, matching and in plane smoothing using an 0.4-mm Gaussian filter (FWHM) (Jonckers et al. 2011). A band pass filter (0.01–0.1 Hz) was applied to the temporal data to rule out low frequency noise. To calculate the functional connectivity, region of interest (ROI)-based analysis was conducted, using "resting state fMRI data analysis toolkit". A correlation matrix was calculated displaying the FC between the regions identified as primary regions of interest by the subchronic phMRI study, including prelimbic cortex, cingulated cortex and the hippocampus. Moreover, the FC between the left and right striatum was assessed as a control; no changes due to treatment were predicted. ROIs were delineated referring the std Paxinos rat brain atlas. Subsequently, the mean time course was extracted within the ROIs, and the linear

correlation between all ROI pairs was calculated as a measure of their FC (four correlations: three between ROIs and one between the control region). For all calculations, motion correction was applied, significantly improving the FC calculations (Kalthoff et al. 2011).

Effect of subchronic memantine treatment was assessed by comparing correlation values in SPSS16.0 (http://www.spss.com/software/statistics/) using a repeated measurements design for a $p < 0.05$.

Diffusion MRI

All preprocessing (realignment, normalisation) and the calculations of the invariant diffusion tensor and diffusion kurtosis-based parametric maps, performed on a voxel-by-voxel basis, were done using in-house custom written MATLAB (The Mathworks Inc., Natick, MA, USA) routines. Prior to diffusion MRI analyses, each diffusion-weighted data were corrected for potential subject motion as well as geometrical eddy current distortions by affinely aligning all diffusion-weighted images to a nondiffusion-weighted reference image. Next, the diffusion gradient directions were rotated correspondingly to preserve the orientation information of the diffusion-weighted data (Leemans and Jones 2009).

More reproducible and consistent delineation of ROIs for further statistical analyses of the diffusion MRI data was facilitated by warping all subjects nonlinearly to a study-specific population-based reference template. To this end, all diffusion-weighted data were initially normalised to an arbitrarily chosen reference dataset by in-house affine co-registration software based on the maximisation of the mutual information (Maes et al. 1997). Residual local image misalignments were afterwards corrected by warping all subjects onto a study-specific population-based diffusion tensor imaging (DTI) atlas using a non-rigid co-registration technique, based on a viscous fluid model (Van Hecke et al. 2008).

In this study, the diffusion kurtosis model was voxel-wise fitted to the normalised diffusion-weighted images to allow a more accurate estimation of the Gaussian, as well as the non-Gaussian diffusion of water molecules (Veraart et al. 2011). A weighted least squares estimator was used to get an estimate of the diffusion tensor and diffusion kurtosis tensor, which quantify the apparent diffusion coefficient and the deviation from Gaussian diffusion, respectively (Jensen et al. 2005). From the tensor information diffusion parameters [fractional anisotropy (FA), axial- (AD), radial- (RD) and mean diffusivity (MD)] and additional diffusion kurtosis parameters [mean- (MK), axial- (AK) and radial-kurtosis (RK)] were calculated; subsequently repeated measures ANOVA and paired sample t test were conducted to test for the treatment effect for the different diffusion parameters.

Pharmacokinetics of memantine

Subjects were sacrificed at the predefined time points (0.5, 1, 2, 4, 7 and 24 h postdose) by decapitation, and blood was collected by exsanguination. The whole brain was rapidly dissected and immediately stored at ≤ -18 °C. Plasma was obtained following centrifugation at 4 °C. After thawing, brain samples were homogenised in demineralised water $(1/9\,w/v)$ under dimmed light conditions. Memantine concentrations in plasma and brain homogenates were analysed by the Bioanalytical Department (Janssen R&D, Beerse, Belgium) by using a qualified research high-performance liquid chromatography with tandem mass spectrometric detection method. The lower limit of quantification was 2.0 ng/ml for the plasma and 20.0 ng/g for the brain. A limited pharmacokinetic analysis was performed on median values using WinNonlin™ Professional (Version 5.2.1). A noncompartmental analysis using the lin/log trapezoidal rule with lin/log interpolation was used for all data.

## Results

PCP- and memantine-induced hyperlocomotion

Acute dose–response testing

No significant differences in LMA were observed across study groups during the habituation phase ($F(6, 66)=1.4$, p=ns) [Table 2 (see Suppl. Material)]. Subsequent administration of PCP (0.63, 1.25 and 2.5 mg/kg, SC) revealed a statistically significant increase versus vehicle treatment ($F(3, 38)=8.5$, $p<0.001$) where only the 2.5-mg/kg dose of PCP showed statistical significance ($p=0.004$). Memantine (10, 20 and 40 mg/kg, IP) showed increased LMA at 20 and 40 mg/kg versus solvent [$F(3, 37)=11.3$, $p<0.001$; Dunnett post hoc $p=0.001$] [Table 2 (see Suppl. Material)]. The effect of the 40-mg/kg dose did not exceed the 20-mg/kg dose, probably due to stereotypic behaviour.

Effect of subchronic PCP or memantine treatment on LMA

No differences were observed among treatment groups during the initial habituation phase [Table 3 (see Suppl. Material)]. Two-way ANOVA on the challenge phase data revealed a main effect for subchronic treatment ($F(3, 63)=29.3$, $p< 0.001$) and for acute challenge ($F(2, 63)=28.4$, $p<0.001$) and also revealed an interaction for subchronic × acute challenge treatment ($F(1, 63)=6.4$, $p=0.014$). Decomposition showed significant effects of acute memantine treatment in both subchronic memantine and subchronic vehicle-treated subjects (both $p<0.001$ for). The LMA response to acute memantine administration in subchronic memantine or subchronic PCP treated rats was significantly higher than in the subchronic

Fig. 2 phMRI results: SPM (*t*) distribution maps representing BOLD signal changes from memantine-treated study groups overlaid on anatomical template image. *Coloured pixels* represent significant T-scores (threshold at *p*<0.05 corrected for multiple comparisons) of signal time course with input test condition (pretest versus posttest injection). *Red* and *blue* represent BOLD increase and decrease, respectively. **a** Statistical significance of 20 mg/kg, IP, acute memantine (*T*>4.42). **b** Statistical significance of 40 mg/kg, IP, acute memantine (*T*>4.44). **c** Statistical significance of 20 mg/kg, IP, subchronic (5 days) memantine (*T*>4.44)
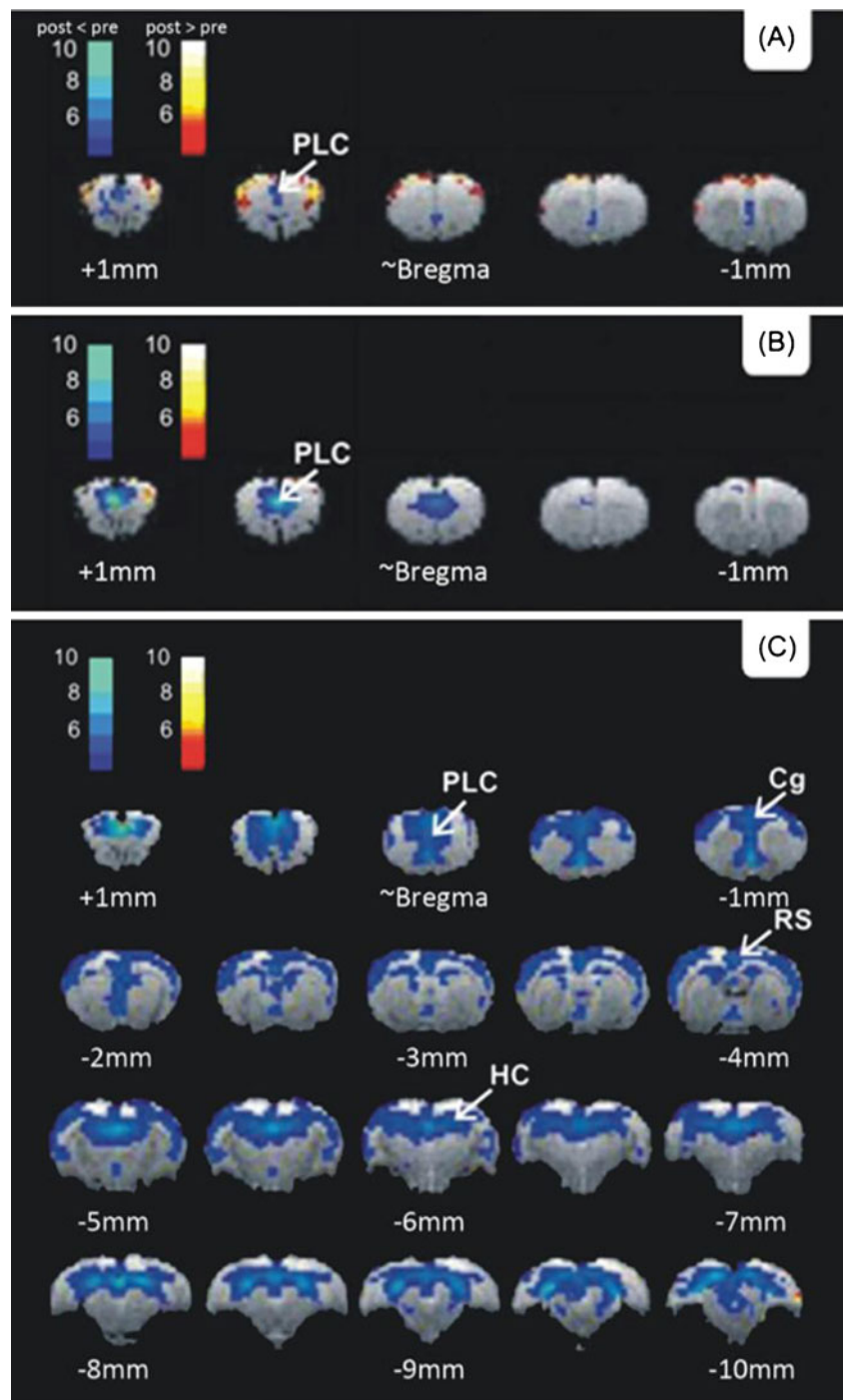
vehicle-treated group (*p*<0.001). Acute memantine administration to subchronic PCP-treated rats also elicited a sensitised LMA response (*p*<0.001) [Table 3 (see Suppl. Material)].

Effect of antipsychotic drugs on LMA in subchronic memantine-treated rats

Memantine-induced hyperlocomotion was dose-dependently reversed by pretreatment with classical antipsychotic drugs (see Suppl. Material).

Pharmacological MRI post acute and subchronic memantine treatment

Voxel-based analysis An acute dose of memantine (20 and 40 mg/kg, IP) produced dose-dependent localised signal increases and decreases in the prelimbic cortex of the brain (for a corrected *p*<0.05, *T*=4.42, and *p*<0.05, *T*=4.44, respectively) (Fig. 2a, b). Following subchronic memantine treatment of 20 mg/kg, IP, significantly localised negative BOLD effects in the hippocampus, cingulate, prelimbic and
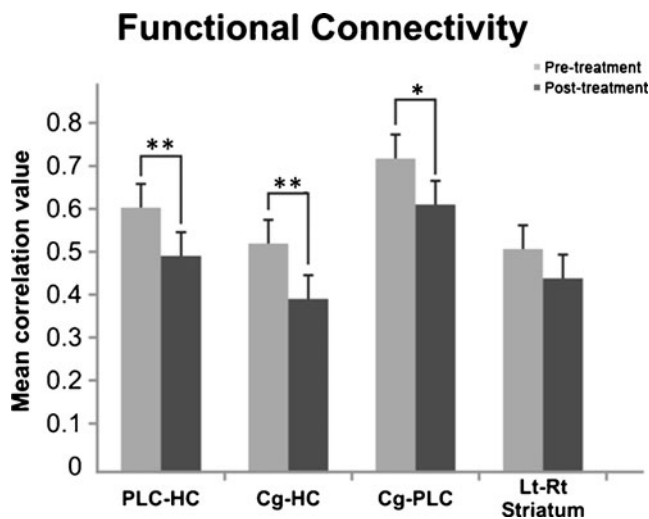
Functional Connectivity

Fig. 3 Resting state functional magnetic resonance imaging results reflecting the strength of functional connectivity between the regions before and after 20 mg/kg IP, subchronic memantine treatment. *PLC*, prelimbic cortex; *Cg*, cingulate cortex; *HC*, hippocampus; *Lt-Rt striatum*, left–right striatum. *Double asterisks* indicate $p<0.01$ and *single asterisk* indicates $p<0.05$ level of significant difference between pretreatment versus posttreatment]

retrosplenial cortices were observed (for a corrected $p<0.05$, $T=4.44$) (Fig. 2c).

Systemic effects To evaluate the confounding nature of the systemic effects within the statistical model, the significance of the covariance of the global muscle signal intensities with the experimental paradigm (the injection protocol) were determined in each treatment group (Lowe et al. 2008). The outcome revealed a nonsignificant covariance with the paradigm [acute memantine 20 mg/kg ($F=1.187, p=0.295$); acute memantine 40 mg/kg ($F=1.137$, $p=0.197$); subchronic memantine 20 mg/kg ($F=3.022$; $p=0.101$)]; hence, the muscle signal intensity changes within these groups may justifiably be regarded as additive nuisance components within the model and not as a confound (Lowe et al. 2008; Sekar et al. 2011a, b).
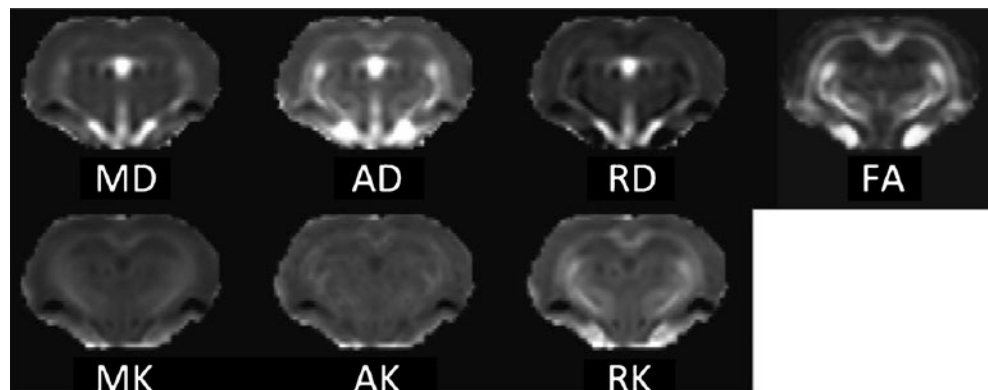
Resting state fMRI following subchronic memantine treatment

Brain regions which showed phMRI functional alterations after memantine treatment were used in a regional analysis of FC changes before and after subchronic memantine treatment (Fig. 3). Decreases in FC were apparent amongst the hippocampus–prelimbic cortex ($F(1, 6)=8.335, p=0.0028$), hippocampus–cingulate cortex ($F(1, 6)=8.314, p=0.0028$) and amongst the cortex (cingulate cortex–prelimbic cortex; $F(1, 6)=8.013, p=0.030$). FC between the left and right striatum (calculated as a negative control; no phMRI change expected) did not reflect a significant change upon subchronic memantine treatment ($p=0.876$).

Diffusion MRI following subchronic memantine treatment and wash-out

Diffusion parameters including MK, RK, AK, MD, RD, AD and FA were extracted from key ROIs (led by phMRI activations including the hippocampus, cingulate, prelimbic and retrosplenial cortex) and striatum (control region). Statistical tests were conducted across the absolute diffusion parameter values of the pretreatment, posttreatment and postwash-out datasets (Figs. 4 and 5).

The outcome of repeated measures ANOVA revealed statistical significant changes of the FA and AD in the hippocampus ($F(2, 12)=4.965, p=0.027$) and ($F(2, 12)=4.665, p=0.032$), respectively. Further AD values from the cingulate cortex also reflected significant changes ($F(2, 12)=4.604, p=0.033$). The rest of the diffusion parameters across all the regions of interest investigated failed to reflect any statistical significant change.

The paired sample t test amongst the pretreatment and posttreatment reflected significant decreases in the FA and AD in the hippocampus: ($t(7, 2.43)=2.953, p=0.021$) and ($t(7, 7.22)=2.79, p=0.027$), respectively, as well as marginal increase for the AD between the posttreatment and postwash-out condition ($t(3, 3.66)=-2.278, p=0.052$).

Fig. 4 DTI/DKI map (diffusion tensor parameters: axial- (*AD*), radial- (*RD*) and mean diffusivity (*MD*); fractional anisotropy (*FA*) and diffusion kurtosis parameters: mean- (*MK*), axial- (*AK*) and radial-kurtosis (*RK*))

Fig. 5 Diffusion kurtosis magnetic resonance imaging results pre and post 20 mg/kg, IP, subchronic memantine treatment and postwash-out. The *asterisk* indicates $p<0.05$ level of significant difference
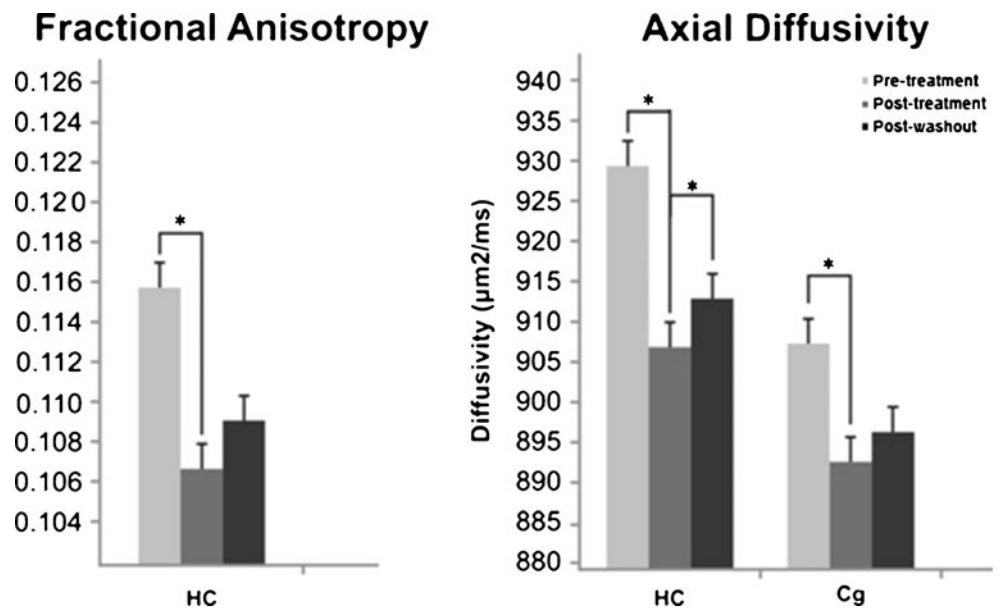
Regarding the cingulate cortex, a statistical significant decrease was observed in the AD between pretreatment and posttreatment ($t(7, 6.2)=2.796$, $p=0.027$).

Pharmacokinetics of memantine

Pharmacokinetics of memantine (20 mg/kg, IP) in the plasma and brain revealed similar exposures (with comparable brain/plasma ratios) between acute and subchronic treatment (Fig. 6). This result validates that the subchronic MRI responses being observed are not a result of differences in drug exposure, but due to the repeated subchronic treatment.
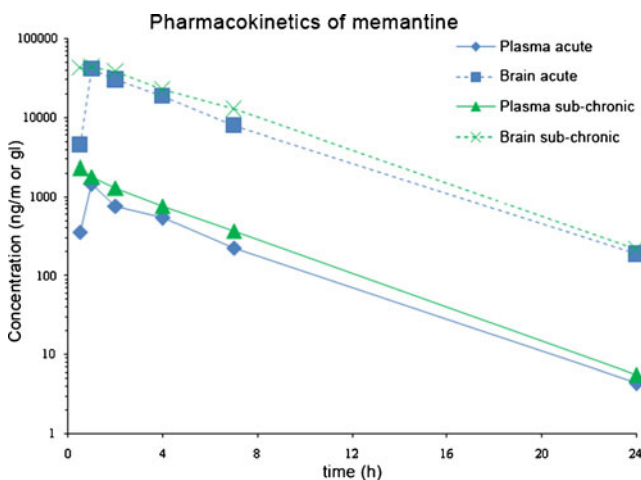

Fig. 6 Pharmacokinetics of memantine at time points of 0.5, 1, 2, 4, 7 and 24 h postinjection (memantine 20 mg/kg, IP); mean data are presented at each time point as $n=3$

Discussion

There is strong preclinical and clinical evidence that NMDA receptor hypofunction models symptoms observed in schizophrenia. We aimed to map the neuroanatomical sites that are involved in the induction of NMDA-mediated changes using neuroimaging methods on rats. Our findings demonstrate the central effects of the noncompetitive NMDA receptor antagonist memantine on brain activation, functional adaptations between acute versus subchronic treatment, as well as its effect after subchronic treatment on brain functional connectivity and ultra-structural tissue integrity in rats.

Memantine-induced hyperlocomotion in naive and subchronically treated rats and its reversal by typical and atypical antipsychotic drugs in the present study is consistent with the literature data describing hyperlocomotion triggered by psychotropic stimulants in rodents (Nagai et al. 2003; Hackler et al. 2010; Ver Donck et al. 2011). This therefore validates the memantine model towards modelling NMDA-mediated psychosis. Acute memantine-induced hyperlocomotion was further enhanced in rats previously treated subchronically for 5 days with memantine. This hypersensitisation to NMDA antagonism is consistent with our earlier findings using subchronic PCP treatment (Ver Donck et al. 2011). Interestingly, reversal of memantine-induced hyperlocomotion by antipsychotic drugs in subchronic memantine-treated rats was observed at doses that did not interfere with spontaneous locomotor activity.

Neuroanatomical target sites of drug action can be mapped using phMRI (Sekar et al. 2011a, b). Acute doses of memantine induced dose-dependent and mainly negative BOLD phMRI responses, primarily in the prelimbic cortex.

Springer

The observed phMRI acute effects diverge from other studies in the direction of the changes (negative BOLD versus positive BOLD) after acute administration of NMDA antagonists such as PCP, ketamine or MK-801 (Gozzi et al. 2008b; Hackler et al. 2010; Littlewood et al. 2006a,b). Moreover, we observed a robust increase in brain glucose metabolism after acute memantine treatment in mice, comparable to acute administration of other NMDA antagonists like ketamine (Dedeurwaerdere et al. 2011). Compared to a single acute memantine dose, subchronic pretreatment with memantine for 5 days resulted in more widespread negative BOLD. The difference observed between acute and subchronic memantine administration cannot be attributed to differences in the plasma and brain exposure as we demonstrated similar pharmacokinetics after acute and subchronic treatment (Fig. 6). In line with these results, most imaging studies find decreased brain activation in rodents and primates following subchronic NMDA antagonist treatment (Cochran et al. 2003; Dawson et al. 2010; Yu et al. 2011). Of note, a negative BOLD response would not necessarily reflect a concomitant decrease in neuronal activity, but could potentially reflect large increases in neuronal activity (Kastrup et al. 2008; Schridde et al. 2008). Though this finding would partially explain the increased brain glucose metabolism reported above, BOLD results are to be interpreted with caution. Our results showing involvement of additional brain regions following subchronic versus acute treatment may indicate that priming the brain with repeated memantine injections may sensitise the brain for a subsequent injection. The prelimbic, cingulate, retrosplenial cortices and the hippocampus were identified as regions of drug action after subchronic memantine treatment. These are potentially vulnerable regions in schizophrenia and are known to be involved in the mediation of cognitive functions in the domains affected in schizophrenia (Tamminga et al. 2006; Williamson and Allman 2012).

Recent studies indicate rs-fMRI to be an effective tool to study the functional signalling pathways in the brain (Jonckers et al. 2011; Krienen and Buckner 2009). Kurtosis MRI, on the other hand, indicates structural modifications in tissue integrity (Kyriakopoulos and Frangou 2009). The regions identified by the subchronic phMRI experiment were used as primary regions of interest for analysis in the subsequent resting state functional connectivity and diffusion kurtosis MRI investigations. This includes the hippocampus, prelimbic and cingulate cortices. Ample clinical evidence demonstrates disrupted functional connectivity within these circuits with rs-fMRI (Meyer-Lindenberg et al. 2005; Lawrie et al. 2002) and EEG studies (Ford et al. 2002) in schizophrenic patients. Following subchronic memantine treatment, there was a significantly decreased resting state FC between the hippocampus and the prelimbic and cingulate cortices. Moreover, decreased FC

was also apparent amongst the latter two brain regions. Recently, impaired hippocampal–prefrontal synchrony has been documented in a genetic mouse model of schizophrenia (Sigurdsson et al. 2010).

Clinical studies in schizophrenic patients have reported fractional anisotropy (FA) reductions (White et al. 2007). With diffusion kurtosis MRI, we demonstrated that FA was affected in the hippocampus in particular, and axial diffusivity (AD) was significantly decreased in the hippocampus and cingulate cortex after subchronic memantine treatment. Moreover, the decreases in AD persisted after a wash-out period of 3 days indicates the long-lasting nature of memantine-induced changes. Our diffusion kurtosis imaging (DKI) results potentially suggest ultra-structural alterations in the hippocampus and the cingulate cortex after 5 days of subchronic memantine treatment at high dose. Whether these structural changes involve axonal degeneration, loss of synapses, oedema, or other changes would require further verification.

The level of anaesthesia used (i.e., 0.9 to 2 % isoflurane) could be a potential confounding factor as it has been demonstrated that changes in anaesthesia can alter the direction of the BOLD response induced by NMDA antagonists (Gozzi et al. 2008a). Therefore, the results are to be interpreted with caution. However, immobilisation of animals during scanning by anaesthesia is still considered the standard method to avoid motion artefacts and the influence of altered stress levels, which can lead to false-positive activation. While the study by Gozzi and colleagues (2008a) suggested 0.8 % of halothane anaesthesia as a cut-off, other studies using PCP (Hackler et al. 2010) or ketamine (Littlewood et al. 2006a) in combination with isoflurane (1 and 1.6 %, respectively) still obtained positive BOLD responses. Though the vast majority of MRI studies are still conducted under anaesthesia, imaging studies in conscious rodents are being endeavoured (Chin et al. 2011; Ling et al. 2011) using dedicated animal holder and acclimation training (King et al. 2005). Such approaches may hold promise for future rodent imaging.

Our multimodal imaging results provide evidence of concurrent decreases in BOLD signal, functional disconnectivity and altered ultra-structural tissue integrity in the prefrontal–hippocampal regions upon subchronic memantine treatment. This would substantiate the hypothesis that repeated NMDA receptor blockade with nonspecific, noncompetitive NMDA antagonists may lead to structural alterations particularly in the hippocampus and cingulate cortex. This study also illustrates the utility of comprehensive multimodal imaging (pharmacological, resting state and diffusion kurtosis MRI) towards the development of noninvasive imaging models.

In addition, it is important to note that memantine is a clinically approved drug, in contrast to its scheduled counterparts such as ketamine or PCP. Therefore, the use of

memantine as a pharmacological challenge model carries a translational potential, as it would be possible to study the effects of memantine in man in well-controlled imaging studies, both following acute and chronic/repeated administration.

References

Areosa SA, Sherriff F, McShane R (2005): Memantine for dementia. The cochrane database for systematic reviews. CD 003154.pub3. 2005

Ashburner J, Neelin P, Collins DL, Evans A, Friston K (1997) Incorporating prior knowledge into image registration. NeuroImage 6:344–352

Alley GM, Bailey JA, Chen D, Ray B, Puli LK, Tanila H, Banerjee PK, Lahiri DK (2010) Memantine lowers amyloid-beta peptide levels in neuronal cultures and in APP/PS1 transgenic mice. J Neurosci Res 88(1):143–154

Bifone A, Gozzi A, Schwarz AJ (2010) Functional connectivity in the rat brain: a complex network approach. Magn Reson Imaging 28 (8):1200–1209, Review

Borsook D, Becerra L (2010) Using NMR approaches to drive the search for new CNS therapeutics. Curr Opin Investig Drugs 11 (7):771–778, Review

Borsook D, Becerra L, Hargreaves R (2006) A role for fMRI in optimizing CNS drug development. Nat Rev Drug Discov 5:411–424

Bubeníková-Valesová V, Horácek J, Vrajová M, Höschl C (2008) Models of schizophrenia in humans and animals based on inhibition of NMDA receptors. Neurosci Biobehav Rev 32(5):1014–1023, Review

Chin CL, Upadhyay J, Marek GJ, Baker SJ, Zhang M, Mezler M, Fox GB, Day M (2011) Awake rat pharmacological magnetic resonance imaging as a translational pharmacodynamic biomarker: metabotropic glutamate 2/3 agonist modulation of ketamine-induced blood oxygenation level dependence signals. J Pharmacol Exp Ther 336(3):709–715

Cochran SM, Kennedy M, McKerchar CE, Steward LJ, Pratt JA, Morris BJ (2003) Induction of metabolic hypofunction and neurochemical deficits after chronic intermittent exposure to phencyclidine: differential modulation by antipsychotic drugs. Neuropsychopharmacology 28 (2):265–275

Coyle JT, Tsai G (2004) NMDA receptor function, neuroplasticity, and the pathophysiology of schizophrenia. Int Rev Neurobiol 59:491–515, Review

Danysz W, Parsons CG, Mobius HJ, Stoffler A, Quack G (2000) Neuroprotective and symptomatological action of memantine relevant for Alzheimer's disease—a unified glutamatergic hypothesis on the mechanism of action. Neurotox Res 2(2–3):85–97

Dawson N, Thompson RJ, McVie A, Thomson DM, Morris BJ, Pratt JA (2010) Modafinil reverses phencyclidine-induced deficits in cognitive flexibility, cerebral metabolism, and functional brain connectivity. Schizophr Bull 38(3):457–474

Dedeurwaerdere S, Wintmolders C, Straetemans R, Pemberton D, Langlois X (2011) Memantine-induced brain activation as a model for the rapid screening of potential novel antipsychotic compounds: exemplified by activity of an mGlu2/3 receptor agonist. Psychopharmacology 214:505–514

Delgado y Palacios R, Campo A, Henningsen K, Verhoye M, Poot D, Dijkstra J, Van Audekerke J, Benveniste H, Sijbers J, Wiborg O, Van der Linden A (2011) Magnetic resonance imaging and spectroscopy reveal differential hippocampal changes in anhedonic and resilient subtypes of the chronic mild stress rat model. Biol Psychiatry 70(5):449–457

Ford JM, Mathalon DH, Whitfield S, Faustman WO, Roth WT (2002) Reduced communication between frontal and temporal lobes during talking in schizophrenia. Biol Psychiatry 51(6):485–492

Fox GB, Chin CL, Luo F, Day M, Cox BF (2009) Translational neuroimaging of the CNS: novel pathways to drug development. Mol Interv 9:302–313

Gilmour G, Pioli EY, Dix SL, Smith JW, Conway MW, Jones WT, Loomis S, Mason R, Shahabi S, Tricklebank MD (2009) Diverse and often opposite behavioral effects of NMDA receptor antagonists in rats: implications for "NMDA antagonist modelling" of schizophrenia. Psychopharmacology 205:203–216

Gozzi A, Herdon H, Schwarz A, Bertani S, Crestan V, Turrini G, Bifone A (2008a) Pharmacological stimulation of NMDA receptors via co-agonist site suppresses fMRI response to phencyclidine in the rat. Psychopharmacol (Berl) 201(2):273–284

Gozzi A, Large CH, Schwarz A, Bertani S, Crestan V, Bifone A (2008b) Differential effects of antipsychotic and glutamatergic agents on the phMRI response to phencyclidine. Neuropsychopharmacology 33(7):1690–1703

Hackler EA, Byun NE, Jones CK, Williams JM, Baheza R, Sengupta S, Grier MD, Avison M, Conn PJ, Gore JC (2010) Selective potentiation of the metabotropic glutamate receptor subtype 2 blocks phencyclidine-induced hyperlocomotion and brain activation. Neuroscience 168(1):209–218

Hlustik P, Noll DC, Small SL (1998) Suppression of vascular artifacts in functional magnetic resonance images using MR angiograms. NeuroImage 7:224–231

Houston GC, Papadakis NG, Carpenter TA, Hall LD, Mukherjee B, James MF, Huang CL (2001) Mapping of brain activation in response to pharmacological agents using fMRI in the rat. Magn Reson Imaging 19(7):905–919

Jensen JH, Helpern JA, Ramani A, Lu H, Kaczynski K (2005) Diffusional kurtosis imaging: the quantification of non-Gaussian water diffusion by means of magnetic resonance imaging. Magn Reson Med 53(6):1432–1440

Jonckers E, Van Audekerke J, De Visscher G, Van der Linden A, Verhoye M (2011) Functional connectivity fMRI of the rodent brain: comparison of functional connectivity networks in rat and mouse. PLoS One 6(4):e18876

Kalthoff D, Seehafer JU, Po C, Wiedermann D, Hoehn M (2011) Functional connectivity in the rat at 11.7T: impact of physiological noise in resting state fMRI. NeuroImage 54(4):2828–2839

Kastrup A, Baudewig J, Schnaudigel S, Huonker R, Becker L, Sohns JM, Dechent P, Klingner C, Witte OW (2008) Behavioral correlates of negative BOLD signal changes in the primary somatosensory cortex. NeuroImage 41(4):1364–1371

King JA, Garelick TS, Brevard ME, Chen W, Messenger TL, Duong TQ, Ferris CF (2005) Procedure for minimizing stress for fMRI studies in conscious rats. J Neurosci Methods 148:154–160

Krienen FM, Buckner RL (2009) Segregated fronto-cerebellar circuits revealed by intrinsic functional connectivity. Cereb Cortex 19 (10):2485–2497

Krystal JH, Karper LP, Seibyl JP, Freeman GK, Delaney R, Bremner JD, Heninger GR, Bowers MB Jr, Charney DS (1994) Subanesthetic effects of the noncompetitive NMDA antagonist, ketamine, in humans. Psychotomimetic, perceptual, cognitive, and neuroendocrine responses. Arch Gen Psychiatry 51:199–214

Kyriakopoulos M, Frangou S (2009) Recent diffusion tensor imaging findings in early stages of schizophrenia. Curr Opin Psychiatry 22:168–176

Langsjo JW, Kaisti KK, Aalto S, Hinkka S, Aantaa R, Oikonen V, Sipilä H, Kurki T, Silvanto M, Scheinin H (2003) Effects of subanesthetic doses of ketamine on regional cerebral blood flow, oxygen consumption, and blood volume in humans. Anesthesiology 99(3):614–623

Langsjo JW, Salmi E, Kaisti KK, Aalto S, Hinkka S, Aantaa R, Viljanen T, Kurki T, Silvanto M, Scheinin H (2004) Effects of subanesthetic ketamine on regional cerebral glucose metabolism in humans. Anesthesiology 100(5):1065–1071

Lawrie SM, Buechel C, Whalley HC, Frith CD, Friston KJ, Johnstone EC (2002) Reduced frontotemporal functional connectivity in schizophrenia associated with auditory hallucinations. Biol Psychiatry 51(12):1008–1011

Leemans A, Jones DK (2009) The B-matrix must be rotated when correcting for subject motion in DTI data. Magn Reson Med 61 (6):1336–1349

Ling Z, King JA, Zhang N (2011) Uncovering intrinsic connectional architecture of functional networks in awake rat brain. J Neurosci 31(10):3776–3783

Littlewood CL, Jones N, O'Neill MJ, Mitchell SN, Tricklebank M, Williams SC (2006a) Mapping the central effects of ketamine in the rat using pharmacological MRI. Psychopharmacol (Berl) 186 (1):64–81

Littlewood CL, Cash D, Dixon AL, Dix SL, White CT, O'Neill MJ, Tricklebank M, Williams SC (2006b) Using the BOLD MR signal to differentiate the stereoisomers of ketamine in the rat. NeuroImage 32(4):1733–1746

Lowe AS, Barker GJ, Beech JS, Ireland MD, Williams SC (2008) A method for removing global effects in small-animal functional MRI. NMR Biomed 21:53–58

Maes F, Collignon A, Vandermeulen D, Marchal G, Suetens P (1997) Multimodality image registration by maximization of mutual information. IEEE Trans Med Imaging 16(2):187–198

Malhotra AK, Pinals DA, Adler CM, Elman I, Clifton A, Pickar D, Breier A (1997) Ketamine-induced exacerbation of psychotic symptoms and cognitive impairment in neuroleptic-free schizophrenics. Neuropsychopharmacology 17:141–150

Mechri A, Micallef J, Blin O, Saoud M, Daléry J, Gaha L (2001a) Pharmacological modulation of the effects induced by ketamine at subanesthetic doses. Therapie 56(5):617–622, Review

Mechri A, Saoud M, Khiari G, d'Amato T, Dalery J, Gaha L (2001b) Glutaminergic hypothesis of schizophrenia: clinical research studies with ketamine. Encephale 27(1):53–59, Review

Meyer-Lindenberg AS, Olsen RK, Kohn PD, Brown T, Egan MF, Weinberger DR, Berman KF (2005) Regionally specific disturbance of dorsolateral prefrontal-hippocampal functional connectivity in schizophrenia. Arch Gen Psychiatry 62 (4):379–386

Nagai T, Noda Y, Une T, Furukawa K et al (2003) Effect of AD-5423 on animal models of schizophrenia: phencyclidine-induced behavioral changes in mice. Neuroreport 14:269–272

Olney JW, Farber NB (1995) NMDA antagonists as neurotherapeutic drugs, psychotogens, neurotoxins, and research tools for studying schizophrenia. Neuropsychopharmacology 13:335–345

Olney JW, Labruyere J, Wang G, Wozniak DF, Price MT, Sesma MA (1991) NMDA antagonist neurotoxicity: mechanism and prevention. Science 254:1515–1518

Parsons CG, Stoffler A, Danysz W (2007) Memantine: a NMDA receptor antagonist that improves memory by restoration of homeostasis in the glutamatergic system—too little activation is bad, too much is even worse. Neuropharmacology 53:699–723

Pawela CP, Biswal BB, Hudetz AG, Schulte ML, Li R, Cho YR, Matloub HS, Hyde JS (2009) A protocol for use of medetomidine anesthesia in rats for extended studies using task-induced BOLD contrast and resting-state functional connectivity. NeuroImage 46:1137–1147

Peskind ER, Potkin SG, Pomara N, Ott BR, Graham SM, Olin JT, McDonald S (2006) Memantine treatment in mild to moderate alzheimer disease: a 24-week randomized, controlled trial. Am J Geriatr Psychiatry 14(8):704–715

Schridde U, Khubchandani M, Motelow JE, Sanganahalli BG, Hyder F, Blumenfeld H (2008) Negative BOLD with large increases in neuronal activity. Cerebr Cortex 18(8):1814–1827

Schwarz AJ, Gozzi A, Reese T, Heidbreder CA, Bifone A (2007) Pharmacological modulation of functional connectivity: the correlation structure underlying the phMRI response to d-amphetamine modified by selective dopamine D3 receptor antagonist SB277011A. Magn Reson Imaging 25(6):811–820

Sekar S, Raley JM, Lowe AS, Sharp T, Sibson NR, Blamire AM, Steckler T, Shoaib M (2010) Mapping of anxiogenic neuronal profiles induced by the GABA inverse agonist FG-7142 and caffeine using pharmacological magnetic resonance imaging. Eur Neuropsychopharmacol 20(1):S23

Sekar S, Verhoye M, Van Audekerke J, Vanhoutte G, Lowe AS, Blamire AM, Steckler T, Van der Linden A, Shoaib M (2011a) Neuroadaptive responses to citalopram in rats using pharmacological magnetic resonance imaging. Psychopharmacol (Berl) 213:521–531

Sekar S, Van Audekerke J, Vanhoutte G, Lowe AS, Blamire AM, Van der Linden A, Steckler T, Shoaib M, Verhoye M (2011b) Neuroanatomical targets of reboxetine and bupropion as revealed by pharmacological magnetic resonance imaging. Psychopharmacol (Berl) 217(4):549–557

Sigurdsson T, Stark KL, Karayiorgou M, Gogos JA, Gordon JA (2010) Impaired hippocampal-prefrontal synchrony in a genetic mouse model of schizophrenia. Nature 464(7289):763–767

Tamminga CA (2006) The neurobiology of cognition in schizophrenia. J Clin Psychiatry 67(Suppl 9):9–13, discussion 36-42

Van Hecke W, Sijbers J, D'Agostino E, Maes F, De Backer S, Vandervliet E, Parizel PM, Leemans A (2008) On the construction of an inter-subject diffusion tensor magnetic resonance atlas of the healthy human brain. NeuroImage 43(1):69–80

Ver Donck L, Duytschaever H, Willems R (2011): Low dose subchronic phencyclidine (PCP) pretreatment potentiates acute PCP-induced hyperlocomotion in adult rats: a model of schizophrenia? Society for Neuroscience, abstract 368.13.

Veraart J, Poot DH, Van Hecke W, Blockx I, Van der Linden A, Verhoye M, Sijbers J (2011) More accurate estimation of diffusion tensor parameters using diffusion Kurtosis imaging. Magn Reson Med 65(1):138–145

Weber R, Ramos-Cabrer P, Wiedermann D, van Camp N, Hoehn M (2006) A fully noninvasive and robust experimental protocol for longitudinal fMRI studies in the rat. NeuroImage 29:1303–1310

White T, Kendi AT, Lehericy S, Kendi M, Karatekin C, Guimaraes A, Davenport N, Schulz SC, Lim KO (2007) Disruption of hippocampal

connectivity in children and adolescents with schizophrenia—a voxel-based diffusion tensor imaging study. Schizophr Res 90:302–307

Wilcock G, Mobius HJ, Stoffler A (2002) A double-blind, placebo-controlled multicentre study of memantine in mild to moderate vascular dementia. Int Clin Pychopharmacol 17:297–305

Williams KA, Magnuson M, Majeed W, Laconte SM, Peltier SJ, Keilholz SD (2010) Comparison of alpha-chloralose, medetomidine and isoflurane anesthesia for functional connectivity mapping in the rat. Magn Reson Imaging 28:995–1003

Williamson PC, Allman JM (2012) A framework for interpreting functional networks in schizophrenia. Front Hum Neurosci 6:184

Winblad B, Jones RW, Wirth Y, Stöffler A, Möbius HJ (2007) Memantine in Moderate to Severe Alzheimer´s Disease: A Meta-Analysis of Randomised Clinical Trials. Dement Geriatr Cogn Disord 24:20–27

Wong DF, Tauscher J, Grunder G (2009) The role of imaging in proof of concept for CNS drug discovery and development. Neuropsychopharmacology 34:187–203

Yu H, Li Q, Wang D, Shi L, Lu G, Sun L, Wang L, Zhu W, Mak YT, Wong N, Wang Y, Pan F, Yew DT (2011) Mapping the central effects of Chronic ketamine administration in an adolescent primate model by functional magnetic resonance imaging (fMRI). Neurotoxicology 33 (1):70–77